Int. J. Electrochem. Sci., 17 **(2022)** Article Number: 221019, doi: 10.20964/2022.10.10

International Journal of
ELECTROCHEMICAL
SCIENCE
www.electrochemsci.org

Effect of cathodic protection potential change caused by alternating current interference on corrosion behavior of X90 steel in 3% NaCl solution

Wei Xu, Yi-long Chen, Li-qiu Chen, Hui Huang[*], *Chang-chun Li*

China Special Equipment Inspection & Research Institute, Beijing, 100029, China
[*]E-mail: huanghui@126.com

Received: 24 June 2022 / *Accepted:* 23 July 2022 / *Published:* 10 September 2022

Cathodic protection (CP) is a key method widely used in corrosion protection of buried pipelines. However, under the condition of AC interference, the cathodic potential on the pipeline will change significantly, which will lead to serious corrosion of the pipeline. In this paper, the corrosion behavior of X90 steel under the changing CP potential caused by AC interference was studied by corrosion rate, corrosion morphology and polarization curve. The results showed that the larger the applied AC current density was, the more seriously the CP potential changed. The general corrosion rate and pitting rate of X90 steel increased linearly with the increase of change degree of CP potential, and the severity of surface corrosion was much greater than under the AC current density, showing the DC corrosion characteristic. The negative deviation of the corrosion potential of X90 steel was positively proportional to the change degree of the CP potential of X90 steel, and the corrosion current density was consistent with the general corrosion rate. Moreover, the anode control degree was much higher than that under the AC current density, which was mainly caused by the increase of galvanic cells on the surface corrosion.

Keywords: CP potential change; AC interference; X90 steel; Corrosion behavior

1. INTRODUCTION

Cathodic protection (CP) is a key corrosion protection technology, widely used in buried steel pipeline. Relevant standards all take the off-potential as the effective criteiron of CP system. However, due to the induced voltage of AC (alternating current) electrified railway or high voltage AC transmission line on the pipeline, the CP potential of the pipeline changes. In most reported researches [1-3], under the AC interference, the CP potential will deviate negatively in -0.85 V (CSE) or positively in lower than -0.95 V (CSE) [4,5].

The interference of AC current will affect the CP effect on pipelines, leading to that the CP effectiveness can not be fully evaluated based on the traditional evaluation criteria of off-potential in -0.85~-1.2 V (CSE, saturated copper sulfate reference electrode). Focused on the influence of AC current on CP effectiveness, there were two different research viewpoints. For the one point [6], under the AC current, although the CP potential in -0.85 V (CSE) or with negative deviation of 100 mV relative to natural potential cannot completely protect the pipeline from corrosion, the affected CP potential will partly prevent the pipeline from corrosion of AC current. Another view [7] believed that the increase of CP current cannot effectively reduce the corrosion rate caused by AC interference, but will increase the corrosion rate. Under this condition, the larger CP current was, the higher the corrosion rate will be. The difference of the above results may be attributed to the different corrosion mechanisms caused by different ion types and pH values in the corrosion environment of pipelines.

AC current may cause a change of CP current density in the CP system when the CP potential was influenced on the feedback point of potentiostat. According to operation mechanism of CP potentiostat, if the long-term reference electrode was affected by the AC interference, the CP potential will deviate. Since the CP potential near the feedback point was generally negative, the CP potential will positively deviate under the AC interference. Under this circumstance, the potentiostat will increase the output current according to the affected CP potential as the evaluation basis, which will result in the over-protection of the pipelines, and furthermore resulting in potential harm to hydrogen embrittlement. Actually, the other point of the pipelines affected by AC current will not influence the CP current density. Therefore, focused on the potentiostatic control to study the influence of AC interference on CP potential is inconsistent with the actual situation.

Field test results showed that the CP potential on the pipeline will change around the set potential due to the instability of the CP system and the change of environment. This change will be more pronounced when there was AC interference. It was pointed out in relevant studies [8-11] that when the CP potential change exceeded a certain range, serious pitting corrosion of pipeline surface will be caused. Therefore, in this paper, the change degree of CP potential on the pipeline under different AC current density was determined. Moreover, the corrosion behavior of pipeline steel under AC current density and changing CP potential was studied through corrosion rate, corrosion morphology and polarization curve, to provide reference for CP settings under AC interference.

2. EXPERIMENTAL SETTINGS

In this paper, X90 steel was adopted as the main research object, and its main components were shown in Table 1. The size of X90 sample was 10×10 mm^2. The protective oil film on the surface of the X90 sample was removed with acetone, anhydrous ethanol and deionized water, respectively, and then dried in a vacuum drying oven for 24 hours. Before the experiment, copper wire was welded on the surface of the X90 sample for electrochemical testing and AC/DC signal application, and epoxy resin was used to seal leaving only one working surface. 800#-1200# sandpaper was successively used for polishing, and metallographic sandpaper was used for polishing to ensure that the surface of the sample was mirror-like.

Table 1. The main components of X90 steel (mass fraction, %)

Element	C	Si	Mn	P	S	Ni	Cr	Nb	Mo	Fe
wt.%	0.043	0.23	1.86	0.0084	0.0016	0.46	0.21	0.038	0.29	Bal.

Figure 1 was the experimental device including AC/DC system and electrochemical tests. In Figure 1(a), two systems namely AC interference system and CP system were included. In the AC interference system, X90 steel and graphite electrode were used as the two poles of the AC source, respectively. Different AC current densities (I_{AC} = 0-100 A/m^2) were applied on X90 steel. In the CP system, the DC source provided cathodic protection for X90 steel, with X90 steel as the negative electrode and Pt electrode as the positive electrode. When no AC interference was applied, the CP potential was set to -1.10 V (SCE, saturated calomel electrode). The interaction between the two systems was eliminated by series capacitors and inductors [12]. The most importantly, a high-precision voltmeter connected was set between the X90 steel and reference (SCE), to record the actual CP potential of the X90 steel under the I_{AC} = 0-100 A/m^2. Figure 1 (b) showed the experimental device for studying the corrosion behavior of X90 steel under the AC current density and changing CP potential, including immersion experiment and electrochemical experiment, in which the AC current density was 0-100 A/m^2, and the applied CP potential was the actual CP potential recorded by Figure 1(a).

In the immersion experiment, the corrosion products on the surface of the samples were removed by standard derusting solution, and the weight loss test was carried out to determine the general corrosion rate under the AC current density and changing CP potential. The max pitting depth was determined by Zeiss microscope, and then the pitting rate was calculated, meanwhile the corrosion morphology was recorded.

In Figure 1(b), the electrochemical tests were applied by three electrode system, in which working electrode (WE) was X90 steel, reference electrode (RE) was saturated calomel electrode (SCE) (through lukin capillary connection, filled with saturated KCl solution), and auxiliary electrode (AE) was inert platinum electrode (Pt).

NaCl experimental solution with mass fraction of 3% was prepared with analytical pure NaCl and deionized water. The whole set of experimental equipment was placed in a constant temperature - humidity container to carry out experiments, reducing the influence of environmental changes on experimental results. The experimental temperature was set at 20℃.

The polarization curves were measured with the scanning potential range of ±250 mV (relative to open circuit potential, E_{OCP}), and the scanning rate of 0.5 mV/s. The PowerSuite software was used for the data analysis.

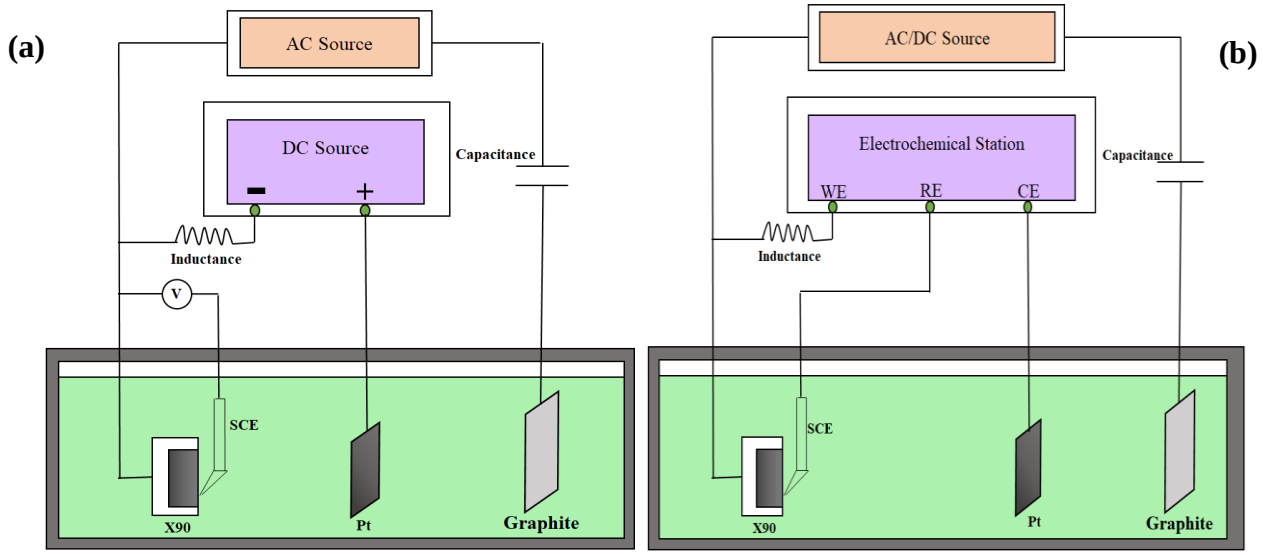

Figure 1. The experimental device including AC/DC system and electrochemical tests: (a) for testing the CP potential of X90 steel under the AC current density in 0-100 A/m^2, and (b) for testing the electrochemical curves of X90 steel under the AC current density and changing CP potential, respectively

3. RESULTS AND DISCUSSION

3.1 CP potential change caused by AC interference

Figure 2 showed the of CP potential change of X90 steel under the AC interference. It can be seen from Figure 2(a) that the CP potential of X90 steel changed irregularly within 600 s around the set CP potential of -1.1 V, and the change frequency did not match the given AC frequency of 50 Hz. In Figure 2(b), with the increase of AC current density, the CP potential of X90 steel changed more and more violently on the basis of -1.1 V. In the range of I_{AC} = 0-60 A/m^2, the positive and negative deviation degrees of CP potential of X90 steel were equal, which were 0.01 V, 0.02 V, 0.05 V and 0.0998 V, respectively. However, with the increase of AC current density, the negative deviation degree of CP potential was greater than the positive deviation degree. When the I_{AC} = 100 A/m^2, the positive deviation was 0.2961 V, while the negative deviation was 0.3990 V, with a difference of 0.1029 V [13,14], indicating that the external AC interference promoted the negative deviation of CP potential [15]. In addition, when the AC current density reached 80 A/m^2, the max deviation of CP potential of X90 steel reached -1.2999 V, which may lead to the hydrogen evolution reaction on the surface of X90 steel, resulting in brittle failure [16].

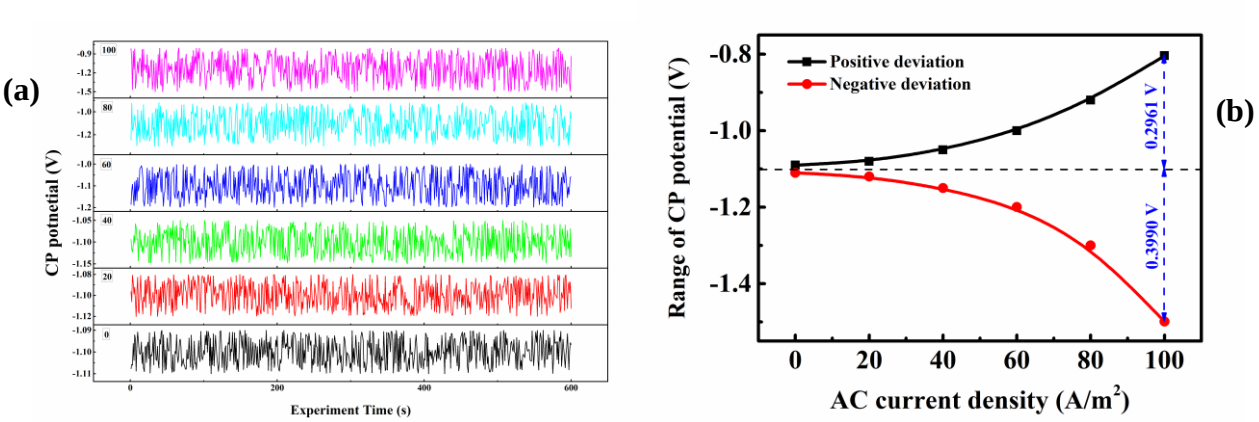

Figure 2. The change curves and range of CP potential of X90 steel under the applied CP potential in -1.1 V and AC current density in 0-100 A/m^2 in 3 wt.% NaCl solution at 25℃: (a) change curves of CP potential of X90 steel within 600 s, and (b) range of CP potential change of X90 steel under the AC current density in 0-100 A/m^2

3.2 Corrosion rate

Figure 3 showed the general corrosion rate and pitting rate of X90 steel under the changing CP potential and AC current density.

Under the AC current density, the general corrosion rate of X90 steel increased with the increase of AC current density, with a decreasing increase rate, satisfying the logarithmic function of v_1-AC=0.1002·ln(I_{AC})-0.0777 (R^2=0.97). Meanwhile, the pitting rate of X90 steel also increased with an increasing increase rate, satisfying the exponential relation of v_2-AC=0.2758·exp[0.0211·I_{AC}] (R^2=0.95) [17]. In above equations, v_1-AC and v_2-AC was the general corrosion rate and pitting rate in mm/a of X90 steel under the AC current density, respectively. Under the changing CP potential, the general corrosion rate and pitting rate of X90 steel increased linearly, namely v_1-CP=0.0057·I_{AC}+0.036 (R^2=0.99) and v_2-CP=0.0274·I_{AC}-0.102 (R^2=0.99). In above equations, v_1-CP and v_2-CP was the general corrosion rate and pitting rate in mm/a of X90 steel under the changing CP potential, respectively. Therefore, it can be seen from the above equations that the corrosion behavior of X90 steel under the changing CP potential caused by AC current density was a Faraday process [18].

Moreover, from the general corrosion rate of X90 steel under the AC current density and changing CP potential, respectively, v_1-AC > v_1-CP in I_{AC} = 0-80 A/m^2, while v_1-AC = 0.55 mm/a < v_1-CP = 0.62 mm/a at I_{AC} = 100 A/m^2. As for the pitting rate, v_2-AC > v_2-CP in I_{AC} = 0-200 A/m^2, while v_2-AC < v_2-CP in I_{AC} = 40-100 A/m^2. This indicated that the pitting behavior of X90 steel was more serious under the changing CP potential [19-22].

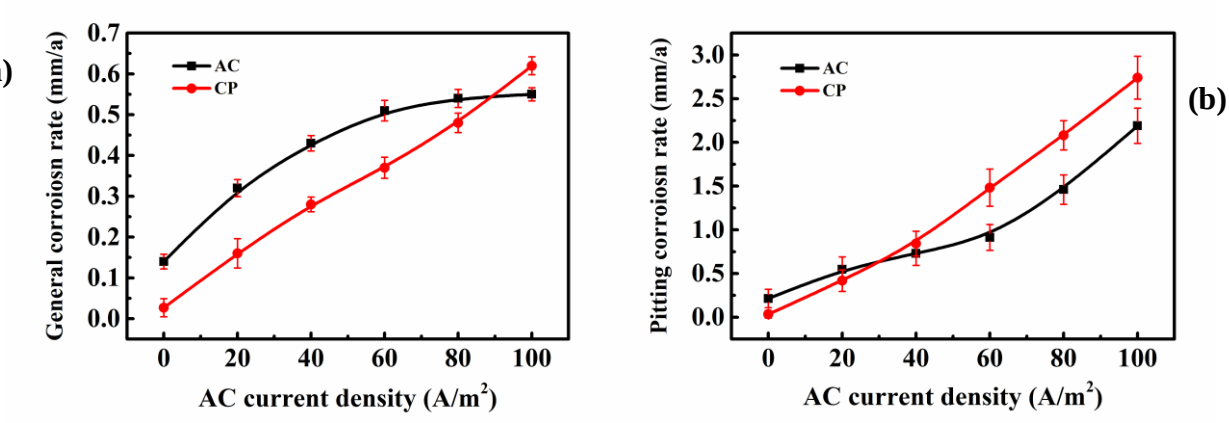

Figure 3. The (a) general corrosion rate and (b) pitting rate of X90 steel under the changing CP potential and AC current density (I_{AC} = 0-100 A/m^2) in 3 wt.% NaCl solution at 25℃

3.3 Corrosion morphology

Figure 4 showed the corrosion morphology of X90 steel under the changing CP potential and AC current density in 3 wt.% NaCl solution at 25℃.

It can be seen from the macroscopic corrosion image Figure 4(1), under the AC current density of I_{AC} = 0-60 A/m^2, X90 steel was mainly comprehensively corroded, and there were a few corrosion pits on the metal surface. The pitting rate in Figure 3(2) increased slightly at this stage. However, in I_{AC} = 60-100 A/m^2, the pitting rate increased rapidly and the pitting pits increased sharply. The corresponding micro morphology in Figure 4(3) showed that under the different AC current density, X90 steel presented pitting corrosion characteristics. However, with the increase of AC current density, the inhomogeneity of metal surface increased significantly and the number of surface corrosion pits increased apparently [23]. In Figure 4(2), under the changing CP potential, a large number of corrosion pits quickly appeared on the surface of X90 steel, and the more serious the CP potential change was, the more corrosion pits were. Furthermore, the number of macro corrosion pits was much larger than that on X90 steel surface under the AC current density [24].

Meanwhile, in Figure 4(4), it can be seen that under the AC current density, the corrosion of X90 steel was slight, and there were only several shallow pits. Once the AC current density was applied, the CP potential changed severely. Under this circumstance, the corrosion pits on X90 steel surface increased obviously with the increase of AC current density, and then the uneven corrosion degree of X90 steel was larger than that under AC current density.

The features of corrosion pits of X90 steel under the different changing CP potential were enlarged, as shown in Figure 4(5). Under the changing CP potential, the surface of small pits was smooth and the edges were neat, showing obvious DC corrosion characteristics. The diameter of corrosion pits increased rapidly from 124 μm to 486 μm under the changing CP potential [25,26], and the corrosion depth was proportional to the AC current density. This was because the irregularly changing CP potential led to the formation of more DC battery in local positions, resulting in the occurrence of more corrosion pits (as shown in Figure 4(4)), and then these pits connected to form a

larger corrosion pit, indicating that with the increase of applied AC current density [27], the more serious the CP potential change was, the larger the size of corrosion pit of X90 steel surface was.

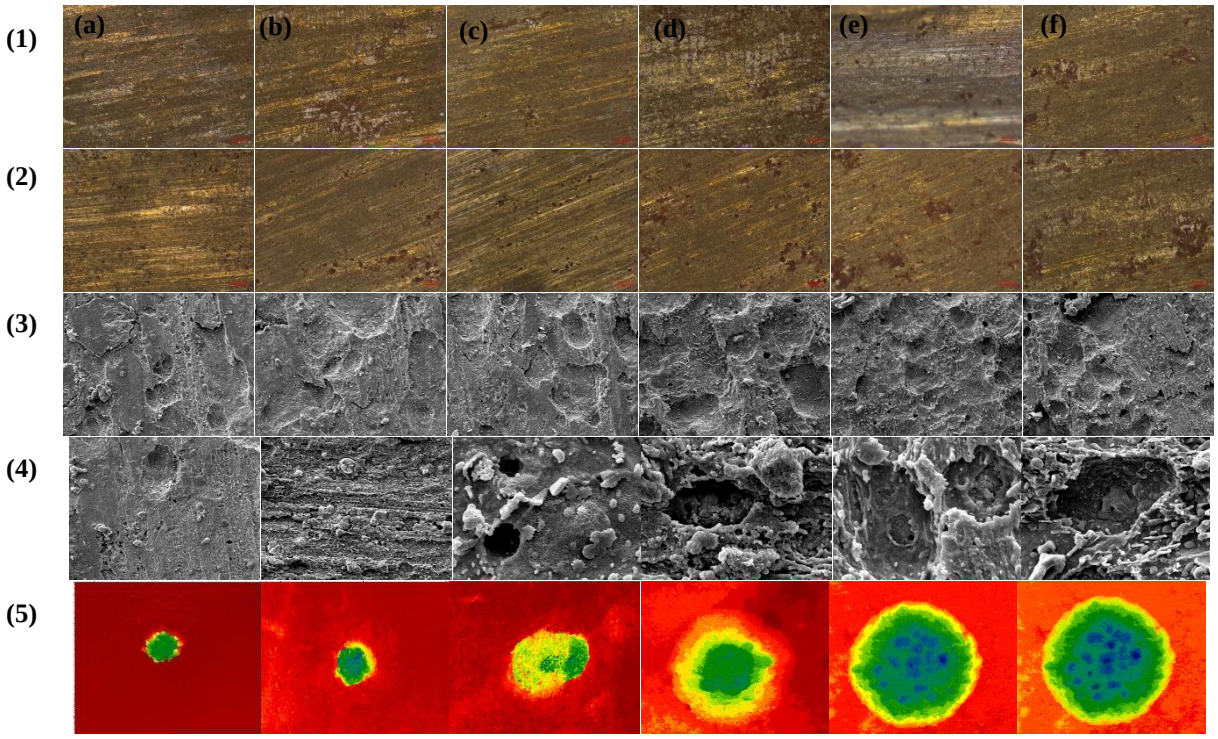

Figure 4. The corrosion morphology of X90 steel under the changing CP potential and AC current density (I_{AC} = 0-100 A/m^2) in 3 wt.% NaCl solution at 25℃: (a)-(f) ~ I_{AC} = 0-100 A/m^2; (1) and (2) was the macro images (×10) of X90 steel under the AC current density and changing CP potential, respectively; (3) and (4) was the micro morphology (×200) of X90 steel under the AC current density and changing CP potential, respectively; (5) was the pits (×1000) of X90 steel under the changing CP potential

3.4 Polarization measurements

Figure 5 showed the polarization curves of X90 steel under the CP potential and AC current density, Table 2 showed the fitting results, and Figure 6 presented the change curves of related parameters.

It can be seen from the polarization curves that the corrosion behavior of X90 steel exhibited active corrosion state under different conditions, and there was no passivation zone on the anodic polarization curve. The corrosion process of X90 steel was analyzed from two aspects of corrosion potential (E_{corr}) and corrosion current density (I_{corr}). Under the AC current density, with the increase of AC current density, the E_{corr} of X90 steel was positively shifted (E_{corr}=0.0017·I_{AC}-0.7137, R^2=0.98), indicating that the corrosion activity increased [28]. Meanwhile, the I_{corr} also increased (I_{corr}=1.0085·I_{AC} +68.597, R^2=0.97), which was consistent with the general corrosion rate in Figure 2(1). The ratio of anode / cathode Tafel constant (r) was all larger than 1, indicating an anode control process. Under the changing CP potential, the more serious the CP potential change on the pipeline was, the greater the E_{corr} of X90 steel was (E_{corr}=-0.001·I_{AC}-1.0991, R^2=0.98), indicating that there was

an increasing hydrogen embrittlement sensitivity of X90 steel. The I_{corr} kept increasing (I_{corr}=53.589·exp[0.0123·I_{AC}], R^2=0.96) and reached 203.96 μm/cm^2 at I_{AC} = 100 A/m^2, which was larger than 160.67 μm/cm^2 under the AC current [29-31]. In addition, under different conditions, the ratio of anode / cathode Tafel constant was always greater than 1 and kept increasing under the increasing AC current density and changing CP potential, indicating an enhancing anode control. Moreover, the degree of anode control under the changing CP potential was much larger than that under the AC current density.

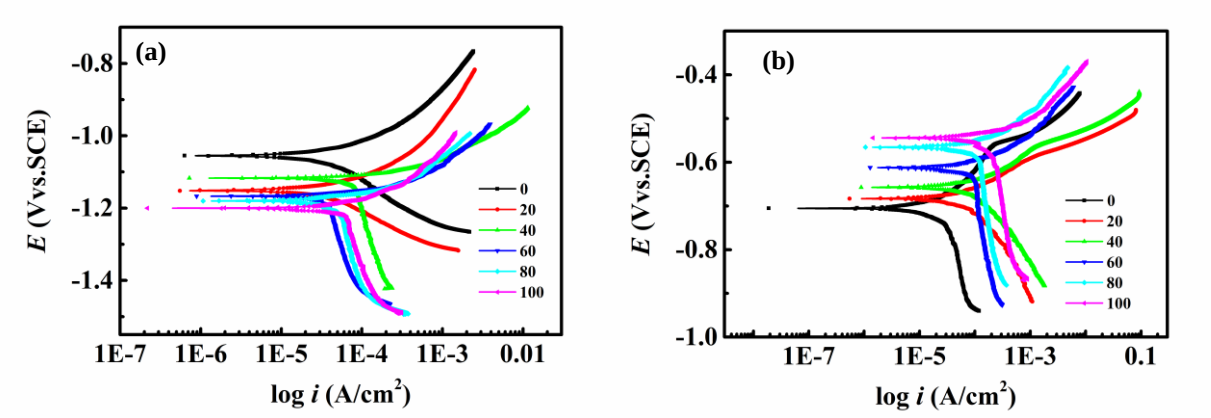

Figure 5. The polarization curves of X90 steel under different conditions in 3 wt.% NaCl solution at 25°C: (a) changing CP potential, and (b) AC current density

Table 2. The fitting results of polarization curves of X90 steel under the changing CP potential and AC current density in 3 wt.% NaCl solution at 25°C

Condition	AC current density (A/m^2)	E_{corr} (Vvs.SCE)	I_{corr} (μm/cm^2)	β_a (mV/decade)	β_c (mV/decade)	$r=\beta_a/\beta_c$
CP	0	-1.102	52.27	190	106	1.787
	20	-1.123	71.09	253	105	2.403
	40	-1.134	91.77	777	38	20.224
	60	-1.152	112.71	842	32	26.180
	80	-1.187	121.32	877	31	28.019
	100	-1.203	203.96	905	29	30.782
AC	0	-0.705	60.40	755	189	3.994
	20	-0.683	90.545	189	93	2.045
	40	-0.657	117.53	183	78	2.345
	60	-0.612	130.59	179	70	2.568
	80	-0.565	154.38	175	64	2.752
	100	-0.544	160.67	156	46	3.369

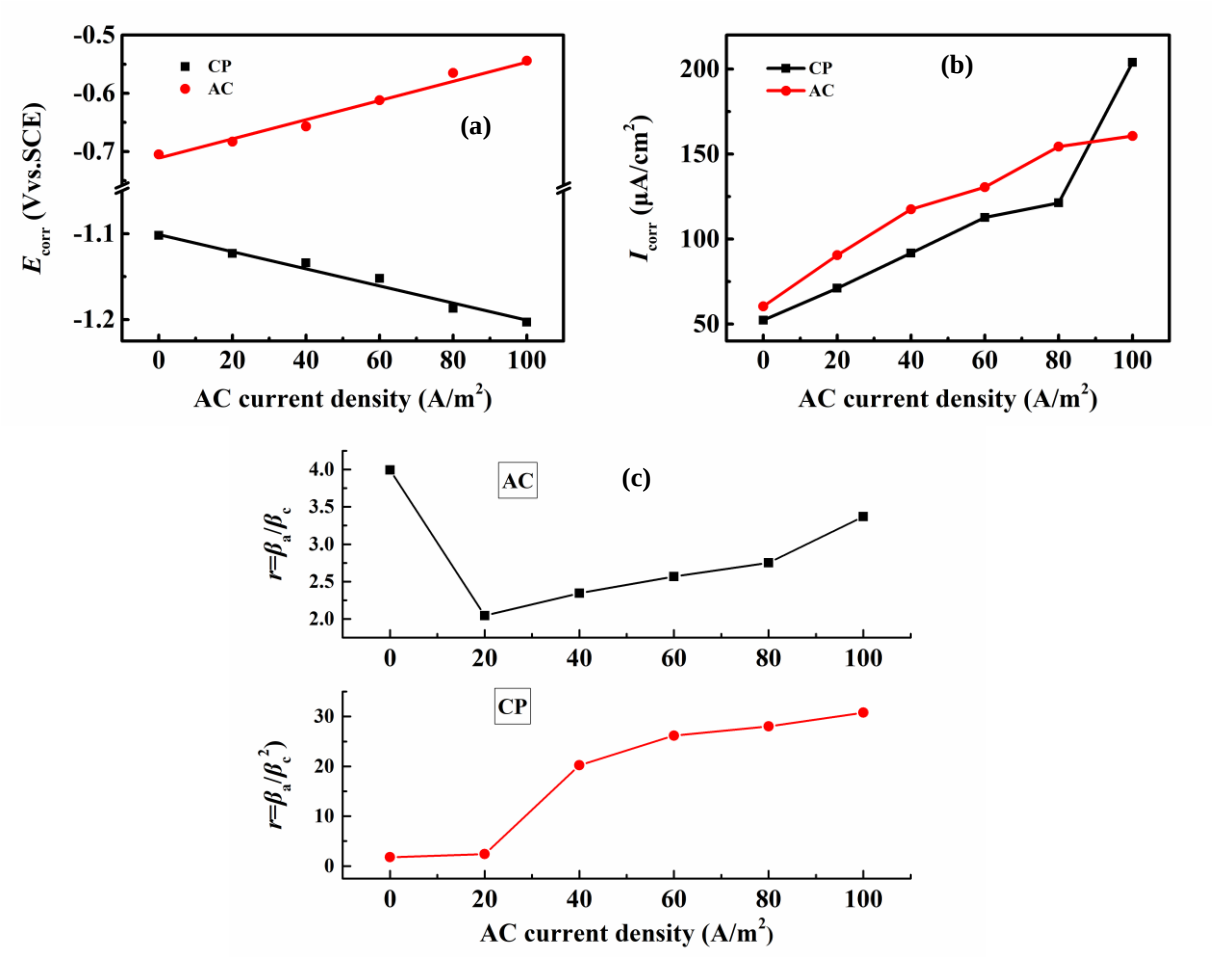

Figure 6. The change curves of related parameters of polarization curves of X90 steel under the changing CP potential and AC current density in 3 wt.% NaCl solution at 25℃: (a) corrosion potential (E_{corr}), (b) corrosion current density (I_{corr}), and (c) ratio of anode / cathode Tafel constant (r)

Therefore, based on the combination of above analysis, it can be seen that with the increase of AC current density, the change degree of CP potential of X90 steel increased. According to the analysis results of corrosion rate and corrosion morphology, the pitting degree of X90 steel under the AC current density was far less than that under the changing CP potential. , and the characteristics of corrosion pits indicated that X90 steel exhibited DC corrosion under the changing CP potential. Furthermore, the corrosion degree of X90 steel was related to the deviation degree of CP potential. The larger the deviation degree was, the more micro corrosion galvanic cells were on the surface, the more serious the anodic control was, and the larger the size of corrosion pit was. Moreover, it should be noted that the more severely the CP potential changed, the more serious the deviation degree of E_{corr} of X90 steel was. Especially when the AC current density increased to 80 A/m^2, the negative deviation degree of CP potential was greater than the positive deviation degree, which may cause the hydrogen embrittlement of X90 steel.

Cathodic protection is one of the key methods to inhibit the corrosion of pipeline, especially for the stray current corrosion. However, the studies in field and laboratory had found that AC interference,

on the one hand, made the traditional CP criterion (-0.85~-1.2 Vvs.CSE) unsuitable, on the other hand, can cause CP potential change [32,33]. Relevant scholars had carried out a large number of studies on the above two aspects and obtained a series of conclusions. As well-known, the corrosion behavior caused by CP change was consistent with the DC corrosion characteristic, as shown in Figure 4. In this paper, it was found that under the set CP potential (CP = -1.1 V), the greater the AC current density was, the greater the difference of positive and negative deviation of CP potential was, and also the corrosion potential (E_{corr}) was negative deviation. Moreover, the corrosion current density (I_{corr}) increased exponentially under the condition of changing CP potential, which was different from the traditional DC corrosion [34-37]. This indicated that the greater the change degree of CP potential was, the greater the increase rate of the corrosion current density was.

4. CONCLUSIONS

In this paper, the corrosion behavior of X90 steel under the CP potential change caused by AC interference was studied by corrosion rate, corrosion morphology and polarization curve. The following conclusions were drawn.

(1) The larger the applied AC current density was, the more seriously the CP potential changed. Furthermore, when the AC current density increased to 80 A/m^2, the negative deviation degree of CP potential was greater than the positive deviation degree.

(2) The general corrosion rate and pitting rate of X90 steel increased linearly with the increase of change degree of CP potential. In general, the general corrosion rate of X90 steel was lower than that under the AC current density, while the pitting rate showed the opposite rule. The severity of surface corrosion was much greater than under the AC current density, showing the DC corrosion characteristic.

(3) The negative deviation of the corrosion potential of X90 steel was positively proportional to the change degree of the CP potential of X90 steel, and the corrosion current density was consistent with the general corrosion rate. Moreover, the anode control degree was much higher than that under the AC current density, which was mainly caused by the increase of galvanic cells on the surface corrosion.

References

1. D. Kuang and Y.F. Cheng. *Corros. Eng. Sci. Techn.*, 52 (2017) 22.
2. L.Y. Xu, X. Su, and Y.F. Cheng. *Corros. Sci.*, 66 (2013) 263.
3. L.W. Wang, L.J. Cheng, J.R. Li, Z. Zhu, S. Bai and Z. Cui. *Materials*, 11 (2018) 465.
4. H.R. Wang, C.W. Du, Z.Y. Liu, L.T. Wang and D. Ding. *Materials*, 10 (2017) 851.
5. M. Ormellese, G. Sara and L. Luciano. *Corros. Eng. Sci. Techn.*, 46 (2011) 618.
6. A.Q. Fu and Y.F. Cheng. *Can. Metall. Quart.*, 51 (2012) 81.
7. M. Buckler and H.G. Schoneich. *Corrosion*, 65 (2009) 578.
8. Y. Liang, Y.X. Du, D.Z. Tang, L. Chen, L. Zhang and L.J. Qiao. *Corros. Sci.*, 197 (2022) 110085.
9. J.L. Wendt and D.T. Chin. *Corros. Sci.*, 25 (1985) 889.
10. S. Goidanich, L. Lazzari and M. Ormellese. *Corros. Sci.*, 52 (2010) 916.
11. A.Q. Fu and Y.F. Cheng. *Corros. Sci.*, 52 (2010) 612.

12. S. Muralidharana, D.K. Kim, T.H. Ha, J.H. Bae, Y.C. Ha, H.G. Lee and J.D. Scantlebury. *Desalination*, 216 (2007) 103.
13. M. Attarchi, A. Brenna and M. Ormellese. *J. Nat. Gas Sci. Eng.*, 82 (2020) 103497.
14. E.M. Shaalan, M.A. Mostafa, A.S. Hamza and M. Al-Gabalawy. *Electr. Pow. Syst. Res.*, 210 (2022) 108064.
15. Y.B. Guo, H. Tan, T. Meng, D.G. Wang and S.H. Liu. *J. Nat. Gas Sci. Eng.*, 36 (2016) 414.
16. M. Ormellese, S. Beretta, F. Brugnetti and A. Brenna. *Constr. Build. Mater.*, 281 (2021) 122645.
17. S. Goidanich, L. Lazzari and M. Ormellese. *Corros. Sci.*, 52 (2010) 491.
18. D.T. Chin and P.J. Sachdev. *Electrochem. Soc.*, 130 (1983) 1714.
19. L.Y. Xu, X. Su and Y.F. Cheng. *Corros. Sci.*, 66 (2013) 263.
20. T.C. Tan and D.T. Chin. *J. Appl. Electrochem.*, 18 (1988) 831.
21. L. Sánchez and H. Cong. *Eng. Fail. Anal.*, 129 (2021) 105661.
22. L. Sánchez, T. Fricker and H. Cong. *Corros. Sci.*, 203 (2022) 110335.
23. C.K. Dyer and R.S. Alwitt. *J. Electrochem. Soc.*, 128 (1981) 300.
24. D.T. Chin and S. Venkatesh. *J. Electrochem. Soc.*, 128 (1981) 1439.
25. M. Srinivasan, K.K. Dae, H.H. Tae, H.B. Jeong, C.H. Yoon and G.L. Hyun. *Desalination*, 216 (2007) 103.
26. S.B. Lalvani and X. Lin. *Corros. Sci.*, 38 (1996) 1709.
27. R.W. Bosch and W. Bogaerts. *J. Electrochem. Soc.*, 143 (1996) 4033.
28. D. Itzhak and T. Ziberberg. *Corros. Sci.*, 21 (1981) 17.
29. J.M. Costa, F. Sagués and M. Vilarrasa. *Corros. Sci.*, 32 (1991) 665.
30. M. Kurose, Y. Hirose, T. Sasaki and Y. Yoshioka. *Eng. Fract. Mech.*, 53 (1996) 279.
31. L.Y. Xu, X. Su, Z.X. Yin, Y.H. Tang and Y.F. Cheng. *Corros. Sci.*, 61 (2012) 215.
32. D. Z. Tang, Y. X. Du, M. X. Lu, Z. T. Jiang, L. Dong and J. J. Wang. *Mater. Corros.*, 66 (2013) 278.
33. M. Markić, S. Arat and W. Fürbeth. *Mater. Corros.*,73 (2022) 45.
34. X. He, G. Jiang, Y. Qiu, G. Zhang, X. Jin, Z. Xiang, Z. Zhang and H. Tang. *Mater. Corros.*, 63 (2011) 534.
35. A. Junker, L.J. Belmonte, N. Kioupis, L.V. Nielsen and P. Møller. *Mater. Corros.*, 69 (2018) 1170.
36. M. Büchler. *Mater. Corros.*, 63 (2012) 1181.
37. I. A. Metwally, H. M. Al-Mandhari, Z. Nadir and A. Gastli. *Eur. T. Electr. Power*, 17(2007) 486.

© 2022 The Authors. Published by ESG (www.electrochemsci.org). This article is an open access article distributed under the terms and conditions of the Creative Commons Attribution license (http://creativecommons.org/licenses/by/4.0/).